Zeitschrift: Eclogae Geologicae Helvetiae
Herausgeber: Schweizerische Geologische Gesellschaft
Band: 96 (2003)
Heft: 1

Artikel: Perturbation of the heat flow by water circulation in a mountainous framework : examples from the Swiss Alps
Autor: Jaboyedoff, Michel / Pastorelli, Sabrina
DOI: https://doi.org/10.5169/seals-169005

0012-9402/03/010037-11
DOI 10.1007/s00015-003-1067-4
Birkhäuser Verlag, Basel, 2003

Eclogae geol. Helv. 96 (2003) 37–47

Perturbation of the heat flow by water circulation in a mountainous framework: Examples from the Swiss Alps

MICHEL JABOYEDOFF [1] & SABRINA PASTORELLI[1,2]

Key words: Alpine chain, exhumation, heat flow density, groundwater circulation, geothermal systems

ABSTRACT

In the Swiss heat flow density (HFD) map (Medici & Rybach 1995), areas with the lowest heat flow values correspond to the alpine highest relief and, often, where the highest uplift values are found. 1D thermal simulations show that the exhumation of metamorphic rocks, and consequently the HFD values, should be higher than those observed, as already proposed by Oxburgh & England (1980). The low HFD values in the Alpine region might reflect large amounts of cold groundwater circulating into the massifs that decrease the internal temperatures. This is confirmed by introducing the effect of water circulation in the 1D thermal model. On the contrary, ascending warm waters with relatively high flow rates can heat the surrounding rocks and consequently induce locally positive geothermal anomalies.

RESUME

La carte des flux géothermiques de la Suisse (Medici & Rybach 1995) indique que les régions de plus faible flux correspondent aux reliefs les plus élevés. Ces zones sont aussi celles où les surrections des massifs alpins sont les plus fortes. Un modèle numérique 1D montre que les valeurs de flux géothermiques observée sont plus faibles que celles obtenues par la simulation, comme l'avaient d'ailleurs déjà proposé Oxburgh & England (1980). Ces faibles valeurs de flux dans les régions alpines sont attribuées aux circulations d'eaux souterraines vers le bas. Cet effet est confirmé par l'introduction de l'effet de la circulation d'eau dans le modèle. La situation inverse peut se rencontrer dans le cas d'eaux ascendantes. Elles peuvent réchauffer les roches dans lesquelles elles circulent et induire des anomalies géothermiques positives.

1. Introduction

The Alpine chain consists of pre-Triassic basement sheets, Mesozoic cover lithologies and flysch sequences that underwent different grades of metamorphism during the Cretaceous and Tertiary orogenies (Steck & Hunziker 1994; Escher & Beaumont 1997 and references therein). The highest metamorphic conditions (amphibolitic facies) were recorded approximately 27–38 Ma ago by the units currently outcropping in the Ossola-Ticino region in the southern Swiss and northern Italian Alps (Wenk & Wenk 1984; Steck & Hunziker 1994; Vance & O'Nions, 1992).

At present, low enthalpy geothermal resources in the Central and Western Alps are represented by both springs (Fig. 1) and inflows in deep Alpine tunnels (Vuataz 1982, 1997; Bianchetti et al. 1993; Rybach 1995). The circulation of thermal waters in a mountainous context like the Alpine chain is generally related to the presence of high permeable zones along which meteoric waters can reach relevant depths and that allow their rapid upflow where morphological and structural conditions are adequate (Martinotti et al. 1999). However, as observed in the Simplon tunnel (Hunziker et al. 1990), the Mont-Blanc Tunnel (Gudefin 1967, Maréchal 1998) and the Piora zone of the Gotthard exploration tunnel (Busslinger 1998; Busslinger & Rybach 1999a, 1999b), large descending flows determine a substantial cooling of the interacting rocks. The "cooling effect" of groundwater circulation on the internal temperatures of a massif was estimated by Oxburgh & England (1980) for the eastern Alps to be approximately 30% of the total Heat Flow Density (HFD).

The aim of this paper is to evaluate qualitatively the effect of water circulation on the present thermal state of the Alpine chain by comparing all available results concerning its geological-metamorphic evolution, geothermal observations and thermal modelling. The difference between the thermal behaviour of the alpine relief that are still suffering uplifts movements

[1] Institut de Minéralogie, Université de Lausanne BFSH-2, 1015 Lausanne, Switzerland. E-mail: michel.jaboyedoff@img.unil.ch
[2] SEA Consulting s.r.l., Via Gioberti, 78, 10128 Torino, Italy. E-mail: pastorelli@seaconsult.it

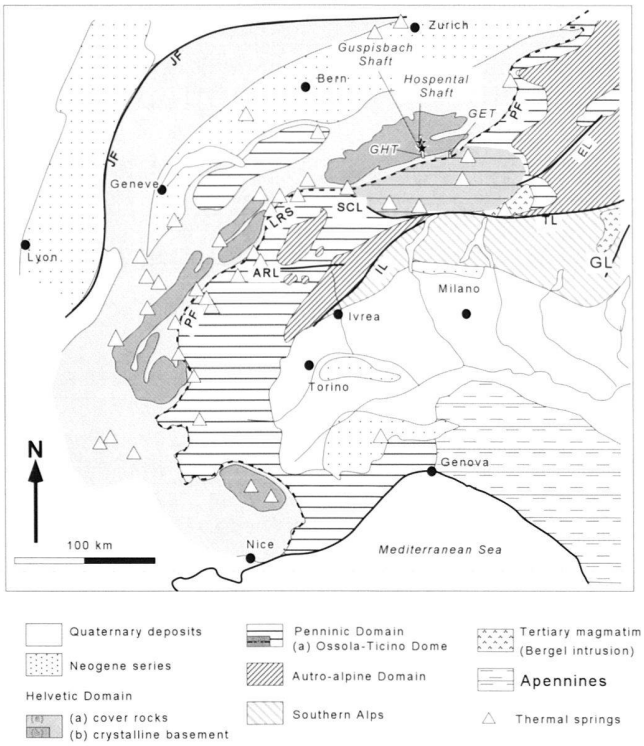

Fig. 1. Geological sketch map of the Western and Central Alps with the location of the main thermal discharges, shafts and tunnels (GHT: Gotthard highway tunnel; GET: Gotthard exploration tunnel; PF: Penninic Front; ARL: Aosta-Ranzola Line; LRS: Rhone-Simplon Line; SCL: Simplon-Centovalli Line; TL: Tonale Line; JF: Jura Front; IS: Insubric Line; EL: Engadina Line; GL: Giudicare Line

and the less disturbed topography, which surrounds the alpine chain is discussed. A simple 1D thermal model that takes into account both the exhumation rates and water circulation is presented in order to evaluate the interaction of subsurface water circulation and heat transfer within a mountainous terrain.

2. HFD values in the Central and Western Alps

A HFD map of Switzerland has been recently prepared by Medici & Rybach (1995) based on temperature data from boreholes, shafts and deep Alpine tunnels. HFD estimations are mainly based on several temperature data or temperature profiles for which topographic and paleoclimatic correction were applied (for details see Medici & Rybach, 1995). This map shows that the regional heat flow decreases toward the south and the lowest HFD values are mostly located in the Alpine region (Jaboyedoff & Pastorelli 1999). Although the HFD map was corrected for topographic effects, a good correspondence exits between the HFD map and the topography over 2500 m a.s.l. (Fig. 2): all HFD values located over 800 m a.s.l. are lower than 90 mW/m^2 (Medici & Rybach 1995). Furthermore, the map of the uplift rates indicates that higher values (>0.8mm/a; Kahle et al. 1997) mainly correspond to the regions with low HFD values and are located within the higher topographic levels (Fig. 3). Unfortunately, data values of HFD and uplift rates are not available for the same location, consequently these values are not directly comparable.

In general in alpine region, the HFD values do not exceed 80 mW/m^2 but are essentially lower than 70 mW/m^2. The Mont-Blanc region represents an exception with one value slightly higher than 80 mW/m^2. The lowest HFD values were recorded in the Ossola-Ticino region (Fig. 3) where the highest grade of Alpine metamorphic rocks crop out (Wenk & Wenk

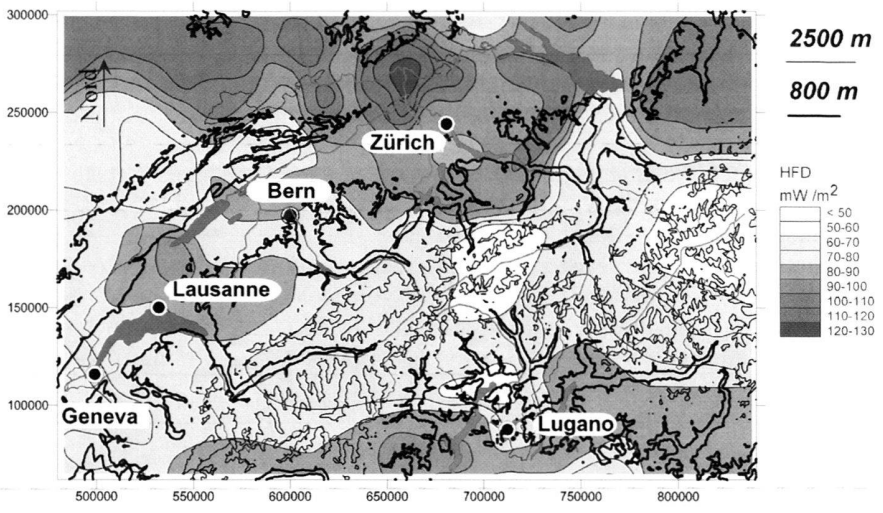

Fig. 2. Comparison of the topographic level 2500 m (bold contour line) and 800 m (fine contour line) with the HFD map. Notice that the higher metamorphic terrains of figure 3 are mostly located below 2500 m, in agreement with the idea of the slow exhumation rates in the recent tectono-thermal history of these terrains.

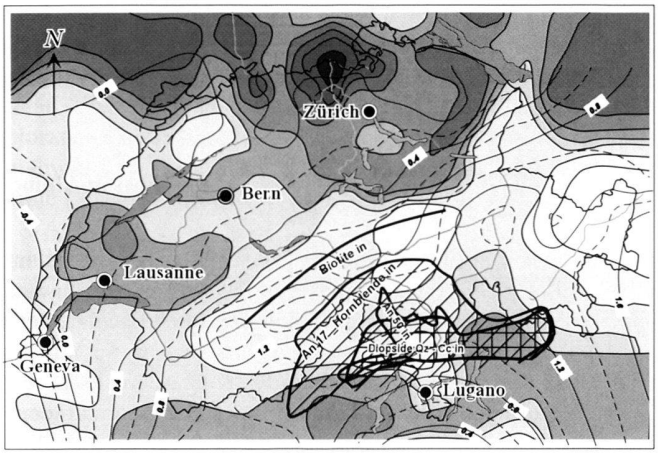

Fig. 3. Comparison of the HFD map corrected for the topographic effect and present uplift rate map in mm/years (after Kahle et al. 1997; Medici & Rybach 1995). The higher grade metamorphic terrains of the Alps, corresponding approximately to amphibolitic facies, are indicated by oblique parallel lines (Wenk & Wenk; 1984; Steck & Hunziker 1994).

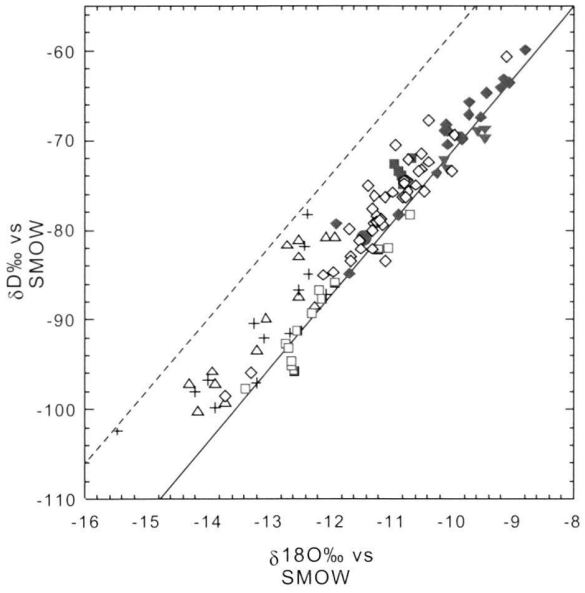

Fig. 4. δD vs. $\delta^{18}O$ diagram. Full line = Worldwide meteoric water line (Rozansky et al. 1993); dash line = Mediterranean meteoric water line for a deuterium excess of 220 (Vuataz 1982). The plotted points represent cold and warm springs as well as water inflows in Alpine tunnels Data from Pastorelli (1999) with the exception of the isotopic values of the springs and the water inflows in the Simplon region, which are taken from Martinotti et al. 1999.

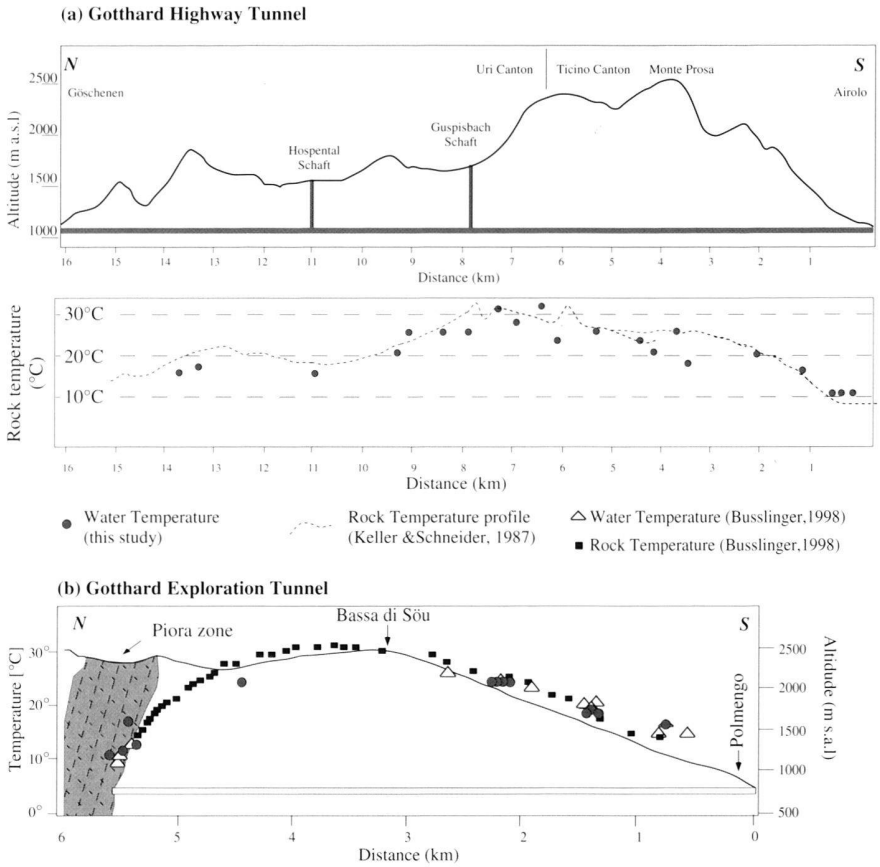

Fig. 5. Cross-sections of the Gotthard highway tunnel (a) and Gotthard exploration tunnel (b) (Pastorelli et al. 2000).

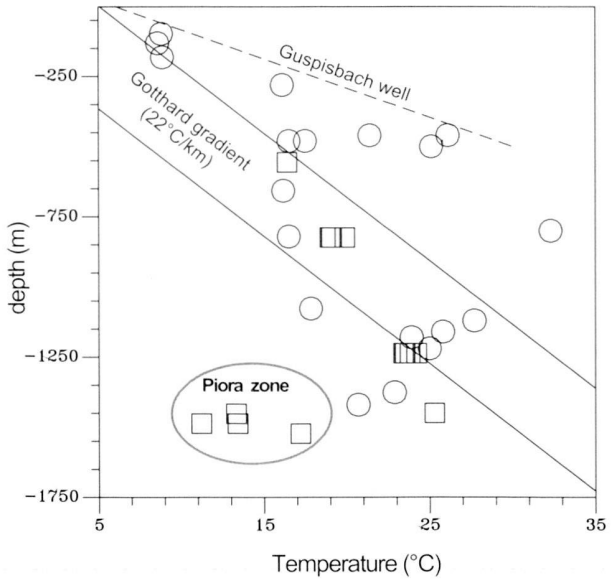

Fig. 6. Plot of water temperatures measured in the Gotthard tunnels vs. depth. The regional geothermal gradient and the temperature vs. depth trend of the Guspisbach well are also shown (Pastorelli et al. 2000). Symbols are as follow: squares = Gotthard exploration tunnel ; circle = Gotthard highway tunnel.

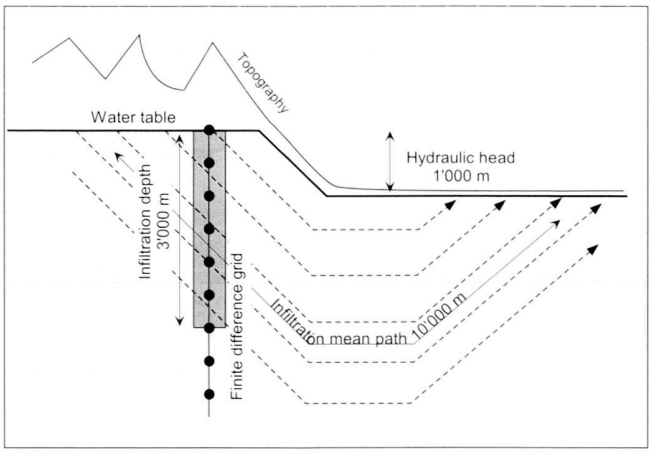

Fig. 7. Description of the thermal model. The fixed grid-nodes are shown, while geological limits are moving through these grid points. The shaded area indicate the zone influenced by water circulation. The schematic flow lines have an average length of 10'000 m.

1984; Steck & Hunziker 1994). During the past 27–38 Ma years, this region underwent a rapid exhumation (~2mm/a) together with a cooling rate up to 30°C/Ma (Steck & Hunziker 1994), while its recent (<2Ma) tectono-thermal history indicates a slower exhumation rate <1mm/a (Grasemann & Mancktelow 1993). The low exhumation rate is also in accordance with the historically reduced seismo-tectonic activity (Pavoni 1977; Maurer et al. 1997; Deichmann et al. 1998) with respect to other sectors of the Alpine chain.

3. Rock-water heat transfer results of water inflows in Alpine tunnels

All available isotopic data (δD, $\delta^{18}O$) on springs and tunnel inflows indicate that the waters circulating in the Alps have a meteoric origin (Fig. 4). These meteoric waters percolate with different velocities through the massifs. Most water inflows into Alpine tunnels are related to descending circuits in low permeable systems. These waters generally have emergence temperatures close to the rock temperatures at the sampling site, suggesting that they approached thermal equilibrium with the rocks (Pastorelli et al. 2000, Fig. 5a). Where large inflows of meteoric waters descend through high permeability channels important cooling effects are caused on the surrounding rocks (Busslinger & Rybach 1999a, 1999b). In these cases, the permeability zones can be related to cataclastic shear zones or layers of dolomitic marbles and anhydrite, where the permeability is controlled mainly by dissolution. Nevertheless, the similarity between the rock-temperature and the water-temperature profiles suggests, again, attainment of water-rock thermal equilibrium (Fig. 5b). This kind of circuits is present in the Simplon tunnel (1000 l/s; Hunziker et al. 1990; Bianchetti et al. 1993), in the Gotthard exploration tunnel (Piora Zone; Busslinger & Rybach 1999a, 1999b) and in the Mont-Blanc tunnel (800 l/s; Gudefin, 1967; Maréchal 1998). In all these cases the regional geothermal gradient is strongly disturbed and low temperatures are measured in both, rocks and waters inflows.

On the opposite, thermal springs and warm inflows in deep tunnels ascend from relatively deep aquifers, which represent potential "geothermal reservoirs". Calculated equilibrium temperatures of these waters are in the range of 30–120°C suggesting that they can reach depths in the order of several km. Discharge temperatures depend on the flow rates of the uprising waters. Uprising warm waters with relatively high flow rates can heat the surrounding rocks and consequently induce unusual high geothermal gradients in the rock pile above the thermal circuit.

The Gotthard massif represents a very interesting case-study of the effects brought about by water circulation on the distribution of the rock temperatures. Based on rock-temperatures measured in the Gotthard railway tunnel, a regional geothermal gradient of 22°C/km was estimated by Clark & Niblet (1956). A similar value, 19°C/km, was obtained by Rybach et al. (1982) elaborating the temperature data of the Gotthard highway tunnel. However, two vertical boreholes (see locations Fig. 1) in the Hospental (300 m) and in the Guspisbach (500 m) areas showed temperature gradients of ~30°C/km and ~50°C/km, respectively, which are considerably higher than the regional geothermal gradient.

In the deep tunnels of the Gotthard massif, the temperatures of most waters are close to the expected values for a regional geothermal gradient of 22°C/km (Fig. 6). However, the relatively large descending waterflows near the Gotthard exploration tunnel termination (Piora Zone) and in the Gotthard highway tunnel (4.0–4.28 km from the southern portal) determine a substantial cooling of the interacting rocks.

According to Bodmer et al. (1979), the high geothermal gradient in the Hospental and the Guspisbach shafts are caused only by a local topographic effect. However, we think that the presence in the Guspisbach zone of ascending warm waters with geothermometrical temperatures of 65–75°C (Pastorelli et al. 2000) is responsible, at least in part for the measured high rock temperatures.

Summing up, water circulation in a mountainous region can strongly disturb the internal distribution of rock temperatures: low geothermal gradients are related to large flows of meteoric waters through highly permeable levels. In contrast, important flows of ascending warm waters can induce higher geothermal gradients than those generally observed in the Alps.

4. 1D thermal model

Method

A 1D finite differential model is used to estimate the effects on HFD of exhumation and water circulation in a mountainous region. The heat production is assumed to decrease exponentially with depth for the basement (Turcotte & Schubert 1982; Čermák & Bodri 1996) and is assumed to be constant at any depth for the sediments. Conductivity, diffusivity, density and heat capacity are kept constant over time and are assumed to be independent of temperature. In order to simulate the thermal state of the Alps, the model assumes a crustal thickening caused by instantaneous thrusting. The points used for the calculations are part of a grid, while the limits of the geological units move inside this grid. For each time-step, the position of the geological units and their properties (thermal conductivity, heat production, etc.) are recalculated for each point of the grid. The model uses the approximation of the 1D heat transfer equation by finite difference (Peacock 1989; Crank 1975; Rybach 1981; Carslaw & Jäger 1959; Incropera & De Witt 1996; Jaboyedoff 2000):

$$\frac{\Delta T}{\Delta t} = \alpha(z,t)\frac{\Delta^2 T}{\Delta z^2} + \frac{\Delta T}{\Delta z}v_z(t) + \frac{A(z,t)}{\rho c(z,t)} - \frac{F(z,t)}{\rho c(z,t)}\frac{\Delta T}{\Delta z} \qquad (1)$$

where Δ denotes the difference between two consecutive grid points, Δ^2 the difference between two consecutive differences, and (z, t) indicate the grid point position at time t. The z values change with time due to the uplift movements. T[K] is the temperature, Δt [s] the increment of time, Δz [m] the spacing between the grid points, α [m^2/s] the rock thermal diffusivity, ρ [kg/m^3] the rock density, c [J/(kgK)] the rock heat capacity, v_z [m/s] the uplift rate (Peacock 1989), A(z) [W/m^3] the rock heat production and F [$W/(Km^2)$] the heat removed by the descending fluid. In the considered pressure-temperature field, fluid is a liquid phase. The erosion is assumed to be equal to v_z in order to have a constant topographic elevation.

The heat absorbed (ω) per unit of time and volume by the water is given by the increase of the water temperature per meter, i.e. the temperature gradient (G) times the water flow (D), heat capacity (c_w) and water density (ρ_w) (Popov et al. 1999):

$$\omega = \rho_w c_w G \times D \times \cos\beta \qquad (2)$$

where β is the angle between the temperature gradient and the water flow. D is given by the Darcy's law: $D = k \times i = k \times h/l$, where i is the adimensional hydraulic gradient, h [m] the hydraulic head, l [m] the length of the water-path and k [m/s] the hydraulic conductivity, taking into account that in our model, G is vertical and D is supposed to be oblique. Therefore, the heat removed in the time unit by the descending fluid from the surface unit per degree Kelvin, F [$W/(Km^2)$], is given by:

$$F = \rho_w c_w \times k \times \cos\beta \qquad (3)$$

The water-flow is assumed to be constant until a given depth where it becomes zero (Fig. 7). Conductivity, heat production and diffusivity data are taken from Bowen (1989), Rybach (1981) and Roy et al. (1981). It must be noted that if we consider 1 m^3 of water heated by all the energy delivered during a year by a heat flow of 80 mW, the temperature of the 1 m^3 water will increase only of 0.6°C.

The model assumes an homogeneous permeable rock mass which is considered equivalent to a fractured media. In the Alps, the rocks are mostly extensively fractured, by small scale fracturing and large scale fracturing. Large open joints allow a rapid velocity transport of water, thus the heat exchange between host rock and water is limited in time and space. On the contrary small-scale joints lead to slower transport velocity allowing a more complete heat transfer and an effect on the whole rock mass. This explanation justifies the assumption of a hydraulic conductivity homogeneous from the whole rock.

Steady state model (no uplift and no erosion)

To evaluate the effect of water circulation on the HFD density, the 1D model is applied to an homogeneous continental crust without uplift and without erosion (Table 1). An initial stationary temperature profile, for an exponential decrease with depth of the heat production, is assumed (Turcotte & Schubert 1982). The values of the calculation parameters are set as: surface HFD = 80 mW/m^2, mantle contribution to HFD = 30 mW/m^2, surface heat production = 2.5 $\mu W/m^3$, thermal conductivity = 2.5 $Wm^{-1}K^{-1}$, thermal diffusivity = $10^{-6} ms^{-1}$ and rock

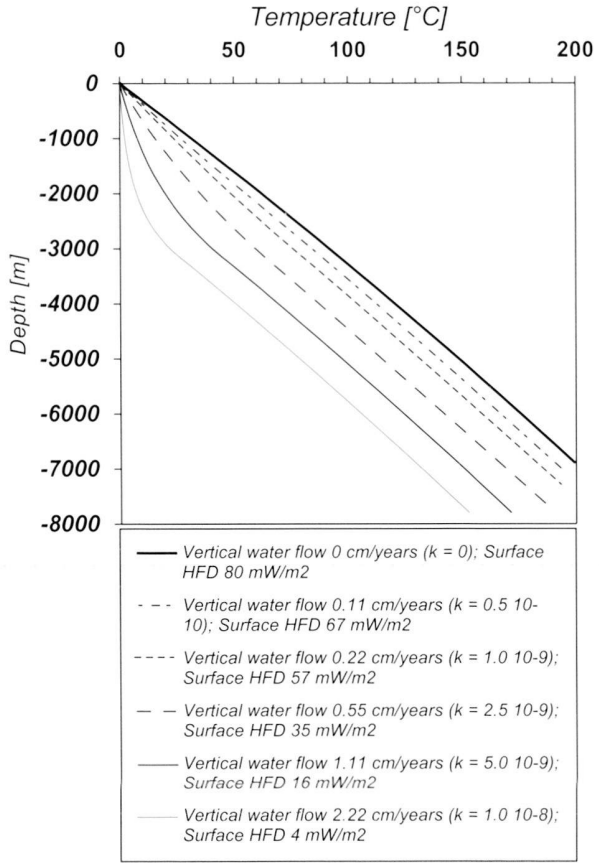

Fig. 8. Temperature vs. depth profile showing the results of the steady state 1D thermal model considering water circulation (see Fig. 7). In particular, in this model it was considered the vertical component od the water flow. The uplift is assumed to be zero (no uplift is considered). The increase of permeability increase the cooling effect. The used hydraulic conductivity k values are 0, 5×10^{-10}, 1×10^{-9}, 2.5×10^{-9}, 5×10^{-9} and 1×10^{-8}m/s.

density = 2750 kg m^{-3}. This relatively high surface HFD value was chosen to obtain high heat production taking into account that the ante-Alpine basement rocks underwent the Hercynian orogeny and suffered magmatic intrusions. The water heat capacity taken is 4180 J $kg^{-1}K^{-1}$ and its mean density is supposed to be 980 kg m^{-3} (Table 1). For convenience, the surface temperature is 0°C. The water inflows reach a depth of 3000 m with linear flow lines at 45° with respect to the vertical temperature gradient. The hydraulic head is 1'000 m and the mean flow line is assumed to be 10'000 m (Fig. 7). The model is applied for different k values (Fig. 8). To provide stability for the computation, the finite difference model consists of a 30 km thick slab and a grid spacing of 300 m with time-steps of 1000 years. The duration of the simulation is 100 Ma in order to reach the stationary temperature profile. The results of the numerical calculation (Fig. 8) show that for a low hydraulic conductivity (0.5×10^{-10} m/s), the water percolation up to a depth

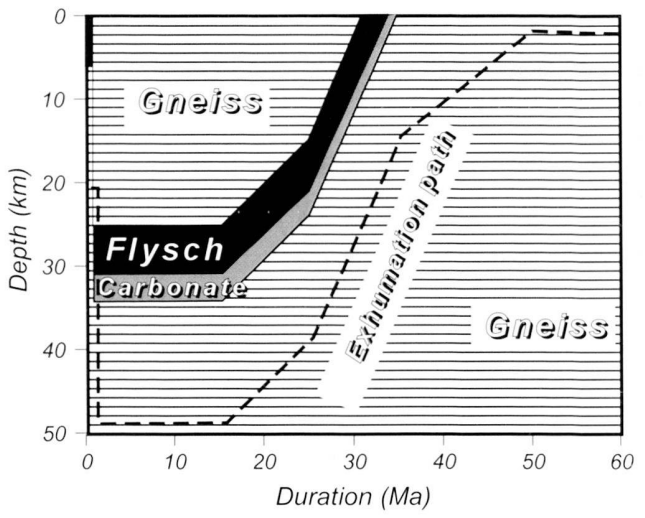

Fig. 9. Time vs. depth profile of the 1D thermal model considering the effect of exhumation process.

of 3'000 m produces a decrease of the surface HFD (80 mW/m^2) in the order of 15%. The considered vertical component of the flow is 0,11 cm/a and it corresponds approximately to 0.1% of the total annual Alpine precipitation (Bodri & Rybach 1998). By using k values up to 2.5×10^{-9}m/s, the calculated HFD values are in agreement with those measured along the Alpine chain. For highest hydraulic conductivity values, the cooling effect appears too important and therefore unrealistic compared to values observed in the Alps (Fig. 8).

Exhumation model by erosion

The geological framework considered (Table 1, Figs. 7 and 9) for the exhumation model is a rock-stack composed of a granito-gneissic basement and its carbonate cover rocks (3 km thick) overlapped by a flysch sequence (6 km thick). The Alpine orogeny is simulated by instantaneous thrusting of a 25 km thick slab of gneissic lithologies at the beginning of the simulation (Fig. 9). The surface temperature for each geological unit is set to 0° C, and the temperature profiles correspond to the upper part of a crust in thermal equilibrium; exception are the carbonates which are in thermal equilibrium with their granito-gneiss basement. For the sedimentary rocks the conductivity is 2 $Wm^{-1}K^{-1}$, while the thermal diffusivity is 1×10^{-6} m^2s^{-1} for the flysch sequence and $0.6\times10^{-6}m^2s^{-1}$ for the carbonates. The rock density is set to 2750 kgm^{-3} for all the three lithologies. The characteristics of the water system are the same as in the previous model. The time increment and Δz are 3000 years and 500 m, respectively. The 50 Ma metamorphic history has been modelled since the thrusting time until the present, according to the geological evolution of the Western and Central Alps (Steck & Hunziker 1994; Escher & Beau-

Table 1. Parameters used for the thermal modelling. For the exhumation model the layer 1 and 2 are in thermal equilibrium.

Steady state model

General parameters

Simulation time:	100 Ma
Step output time:	5 Ma
Time step:	1000 Years
Depth step:	300 m
Density:	2750 kg/m3
Surface temperature:	0 °C

Erosion parameters

N	Start time [Ma]	Speed erosion [mm/year]
1	0	0

Layer parameters

Number of layer: 4

Layer number	Thickness [m]	Number of nods	Thrusting time [Ma]	Diffusion [mm²/s]	Conductivity [W/°K]	$\rho_o Cp$ [J/(°K m³)]	Basal HFD [mW/m²]	Initial surface HFD [mW/m²]	Heat production [μW/m³]	Heat production distribution
1: granito-gneiss	30000	101	0	1	2,5	2500000	30	80	2,5	*Exponential*

Exhumation model by erosion

General parameters

Simulation time:	80 Ma
Step output time:	3 Ma
Time step:	3000 Years
Depth step:	500 m
Density:	2750 kg/m3
Surface temperature:	0 °C

Erosion parameters

N	Start time [Ma]	Speed erosion [mm/year]
1	15	1
2	25	2,5
3	35	0,8
4	50	0

Layer parameters

Number of layer: 4

Layer number	Thickness [m]	Number of nods	Thrusting time [Ma]	Diffusion [mm²/s]	Conductivity [W/°K]	$\rho_o Cp$ [J/(°K m³)]	Basal HFD [mW/m²]	Initial surface HFD [mW/m²]	Heat production [μW/m³]	Heat production distribution
1: granito-gneiss	30000	61	0	1	3	3000000	30	65	2,5	*Exponential*
2: Carbonates	3000	7	0	0,6	2	3333333	0	-	0,6	*Constant*
3: Flysch	6000	13	0	1	2	2000000	15	-	3	*Constant*
4: Granito-gneiss	25000	51	1	1	3	3000000	30	65	2,5	*Exponential*

mont 1997). Uplift and erosion rates are assumed to be equal and correspond therefore to the exhumation rate. The latter is set to 0 for the first 15 Ma, which correspond to the subduction phase (subduction velocity of 0.5 cm/a with an angle of 25° and ~ 30 km of buried crustal material). Afterwards, exhumation processes start and the total exhumation will attain 47 km (Steck & Hunziker 1994; Escher & Beaumont 1997), taking into account an average exhumation rate of: (1) 1 mm/a between 15 and 25 Ma, (2) 2.5 mm/a between 25 and 35 Ma, and (3) 0.8 mm/a between 35 and 50 Ma. The 10 Ma of fast exhumation (2.5 mm/a between 25 and 35 Ma) may correspond to the highest exhumation velocity produced during the collision phase. From 50 Ma to 80 Ma the exhumation rate is set again to zero in order to show the decrease in HFD after the end of the exhumation process. In order to show the decrease of HFD when the exhumation stops, 30 Ma are added to the simulation time. The resulting path is a reasonable approximation of the P-T-t path of the Alps.

Results of the numerical simulation

In a first simulation, the influence of water circulation is not taken into account and therefore a pure conductive surface HFD model is considered (Fig. 10a). Considering exhumation processes, the terrestrial HFD varies with time, and the highest values correspond to the highest exhumation rates (Fig. 11). Before the thrust event, the HFD value is approximately 65 mW/m^2. The cooling effect induced by the thrusting leads to a minimal value of 50 mW/m^2. An exhumation rate of 1 mm/a produces an increase in HFD, which reaches values >80 mW/m^2. If the exhumation rate is higher, a further HFD increase is observed up to 150 mW/m^2. The end of the exhumation process leads to a rapid decrease (9 Ma) of HFD values from 130 mW/m^2 to approximately 100 mW/m^2, and to around 85 mW/m^2 after 30 Ma. More than 100 Ma are necessary to reach the initial HFD conditions in the first 30 km of the crust. This purely conductive model clearly shows that for exhumation rates higher than 1 mm/a the terrestrial HFD values are expected to be above 100 mW/m^2. The HFD obtained through this simulation are of the same order of magnitude of those of Grasemann & Mancktelow (1993), which were calculated using an exhumation model based on normal faulting and erosion. Furthermore, replacing the variable exhumation rate of the previous model by a constant exhumation rate of 1 mm/a, the HFD reaches a value of 130 mW/m^2 at the end of the uplift history.

In a second simulation, water circulation was added to the previous exhumation history. Two different permeability conditions were considered by using at first hydraulic conductivity of $k=10^{-9}$ m/s and then $k=2.5\times10^{-9}$ m/s. This model is qualitative since during the calculations the hydraulic head, the k value and the flow path length were considered constant.

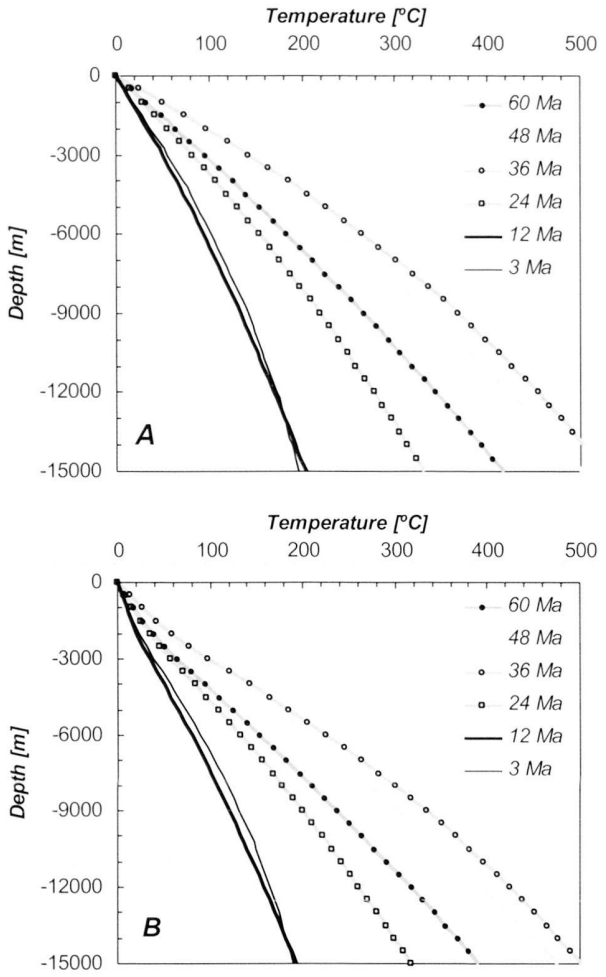

Fig. 10. Evolution of the depth-temperature profiles with time for an infiltration mean-path of 10'000 m as was considered in the models described in figures 7 and 9. A) Purely conductive model. B) With water circulation for a hydraulic conductivity of 2.5×10^{-9}m/s.

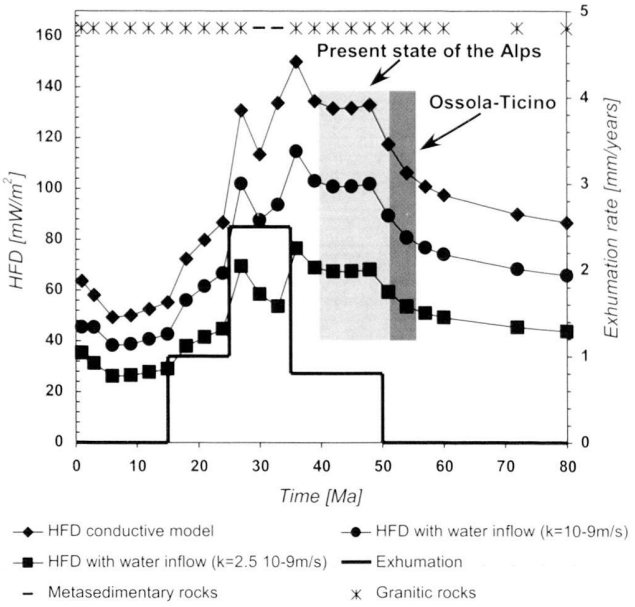

Fig. 11. Evolution of the superficial HFD values with time and associate exhumation rates, for a purely conductive system (diamonds) and for water-circulating systems considering two different permeability conditions: $k=10^{-9}$m/s (full circles) and 2.5×10^{-9} m/s (squares). The geological framework considered is a rock-stack composed by a granito-gneissic basement and carbonate cover rocks (3 km thick) overlapped by a flysch sequence (6 km thick). The thermal conductivity and the diffusivities are 3 $Wm^{-1}K^{-1}$ and 1 mm^2s^{-1}, respectively, for the granitic basement. The conductivity is 2 $Wm^{-1}K^{-1}$ for sedimentary rocks and the diffusivity is 1 mm^2s^{-1} for the flysch and 0.6 mm^2s^{-1} for the carbonates. In this plot, the present situation of the Central Alps can be located in the time-range situated between 40–50 Ma.

For $k=10^{-9}$ and 2.5×10^{-9} m/s the HFD values are 25% and 50% respectively lower than those obtained with the purely conductive model, in agreement with the estimations of Oxburgh and England (1980) for the Eastern Alps. Furthermore, assuming a positive correlation between the uplift rate and the high topographic relief, as it was proposed by Pinet & Souriot (1988), the cooling effect is increased due to the increase in the hydraulic gradient. As a consequence, at the beginning and at the end of the simulation the cooling effect should be smaller than that calculated. Nevertheless, because of the uncertainties in the initial conditions, this approximation is acceptable for our purposes. The most important observation is that, for reasonable k values, the high HFD values of the purely conductive model are decreased due to water circulation leading to HFD values comparable to those measured in the Alps. A further interesting feature of the simulated temperature vs. depth profile (Fig. 10b) is the concave shape of the curves induced by water circulation is, similar to what is observed in the steady state model. A similar temperature vs. depth profiles was also measured in the deepest drill-hole in the world (12'261m) located in the Kola Peninsula, Russia (Popov et al. 1999), even if the hydraulic gradient is smaller than that considered in our model. It must be stressed that this effect is found at greater depths than the cooling effect of the glaciations, which corresponds to few hundred of meters (Medici & Rybach 1995).

5. Discussion

All available geological, HFD and geochemical data as well as the thermal modelling results confirm the hypothesis that a remarkable cooling effect of the Alpine massifs is brought about by water circulation. The purely conductive 1D thermal modelling described here indicates that the HFD values in the Alpine region should be higher than those observed, which are generally below 100 mW/m^2. This value corresponds to a maximum geothermal gradient of 33°C/km for a thermal conduc-

tivity = 3 $Wm^{-1}K^{-1}$. However, introducing water circulation in the model for hydraulic conductivities of 10^{-9} and 2.5 10^{-9}m/s, in the model the resulting heat flow values are ~100 mW/m^2 and ~70 mW/m^2 respectively. These values are in agreement to the ones observed in the Western and Central Penninic Alps. In addition, the model points out that changes of less than one order of magnitude in the hydraulic conductivity (k) may change drastically the thermal behaviour of the massifs, as demonstrated by the depth-temperature profiles (Figs. 8 and 10).

The parameters used for the calculations (k, α, etc.) must be understood as mean values. The infiltration water required for the model (0.1% of the total Alpine precipitation) represents a reasonable fraction of the Alpine average precipitation (Bodri & Rybach 1998). For more detailed investigations into this subject, the flow should vary with depth and 2D models are necessary to take into account the flow-path. However, in this first and simple approach to thermal modelling, the orders of magnitude obtained by the „water cooling effect" coincide with those given by other authors (e.g. Popov et al. 1999; Smith & Chapman 1983). In particular, our model agrees with the observations of Popov et al. (1999), who demonstrated, by detailed analysis of borehole data and by simple thermal modelling, that the meteoric water circulation can disturb the field temperature at least in the first two kilometres of the crust. In accordance to observations made for the Kola SG-3 well, the present model gives a concave-shape temperature-depth profile, which is attributed to the cooling effect of descending waters.

Evidence of deep circulation of meteoric waters down to 4-5 km is provided by the equilibrium temperatures calculated for the thermal springs. The permeability necessary for those circulations is related to brittle tectonic structures, which are located in the first ~10–15 km of the crust (Sibson 1977; Martinotti et al. 1999; Deichmann 1992). Efficient groundwater circuits are probably maintained by fracturing resulting from tectonic movements. For the high topographic levels that are in regions with low HFD values, tectonic activity is suggested by high uplift rates and seismic activity. Due to assumed elevated hydraulic head, important water flows are generated and produce a relevant cooling of the massif.

At present, the Western and the Central Penninic Alps are still affected by differential exhumation processes (Kahle et al. 1997; Steck & Hunziker 1994) (Fig. 11). Assuming that in the simulation the time-range from 40 to 50 Ma corresponds to the present state of the Swiss Alps, and that the 50–55 Ma range is related to the Ticino-Ossola region (Fig. 11), the model can explain the different heat flow values measured in different sectors of the Alpine chain. Even if our model interest the internal part of the Alps, results may give some indication to the more external part of the alpine chain, if higher exhumation rates are considered for the last 5 Ma (at least 1 mm/year higher than the values assumed in our model), which is in accord with the exhumation model of the Helvetic nappes proposed by Burkhard (1990).

Even if the data used to establish the HFD map (Medici & Rybach 1995) are not homogeneously distributed over the Alpine region, our model gives a realistic image of the possible thermal behaviour of the Alps correlated with the deep groundwater circulations. The effect of groundwater circulation seems limited where the topographic levels are lower and where exhumation and seismic activity are reduced, like in the Ossola-Ticino region. In these cases, the HFD values are low, because of the low exhumation rates. This is supported by the observation of Escher et al. (1997), which indicates a crustal-thickness of around 30 km similar to the one of a stable region: therefore the potential of erosion is limited (Burbank & Anderson, 2001). As mentioned before, similar cooling effects (affecting the upper crust) have been identified in the first 2 km of the SG-3 well in Kola peninsula (Popov et al. 1999; Kukkonen & Clauser 1994): 20 mW/m^2 are extracted by water circulation produced by a topographic slope of around 1%. Furthermore, Smith & Chapman (1983) have demonstrated by simulations that with a sufficient hydraulic head the main cooling process is by advection.

Other thermal effects must be invoked to depict the HFD distribution in the Alps. The discharge of ascending warm water circuit at the bottom of the valleys may contribute to an increase of the local HFD compared to the nearby areas. In addition, the topographic effect on the temperature field by conduction must be taken into account (Mancktelow & Grasemann 1997; Rybach & Pfister 1994). Moreover, along normal fault zones, fast exhumation rates might induce high HFD values by thermal conduction. The Simplon fault region is a good example (Grasemann & Mancktelow 1993), and high heat flow values (~ 92 mW/m^2) were calculated in the Simplon Tunnel (Clark & Nibblet 1956). The relatively high HFD value near the Mont-Blanc massif (Seward & Mancktelow 1994) might be explained by a similar situation along the Penninic frontal thrust.

Our model is in contradiction with the model of cooling crust by subduction. The thermo-kinetic model (Okaya & al., 1996) and the map of Medici & Rybach (1995) are in good agreement for an eastern Alps transect. But in this case the cooling produced by the subducted lithosphere mainly causes the relative lowering of HFD values. This leads to a fundamental question: Is the cooling effect caused by water or deep structures? All the thermal data from deep boreholes and deep tunnels confirm that the effect of the water circulation in the Alpine massifs is important and perturb the internal thermal state of the massifs. Certainly, the cooling effect of deep lithosphere during the subduction phase is also important. But during the collision, the angle of subduction increases and finally the deepest part of the crust detached (Stampfli et al., 1998) leading to a new thermal regime. This beginning of an explanation has the advantage to potentially conciliate both theories, if a simple subduction thermal model is invoked.

The good correspondence among the thermal modelling results and geological, geochemical and HFD data, indicates that the hydraulic conductivity values used for calculations (k

of 10^{-9} to 2.5 10^{-9} m/s) are realistic estimations for the mean hydraulic conductivity values of the alpine rocks. The questions are to know if it is small-scale fracturing instead of large permeable systems that mainly controls the permeability of the massif and thus if the used equivalent hydraulic conductivities are relevant? If the cooling effect is accepted as widespread effect in the Alps, the highly permeable zones may be considered as collectors of water coming from the whole-rock mass or the cooling effect will be restricted to the highly permeable zones. These problems are of primary importance for geothermal prospecting in the Alps because if this is true a geothermal system must be formed by a reservoir (small-scale fractured rock mass) and a collector of water by high permeability zones such as important faults or very permeable rock units.

6. Conclusion

The high topographic levels of the Alps are areas, which are probably cooled down by meteoric water circulation inside the massifs, while the bottom of the valleys or minor depressions may be slightly heated, compared to the relief. These conclusions are in agreement with the observations of Bodri and Rybach (1998).

Despite the simplicity of the presented model, the effect of descending waters circulation depicts a coherent picture of the Alpine HFD map (Medici & Rybach 1995). Our model underlines a diminution of the HFD value from 0–50% as already suggests by Oxburgh & England (1980). This fact should be taken into account for recent thermal history studies such as fission track analysis or Alpine isotherms estimation.

Acknowledgements:

We particularly thank Prof. A. Escher and Prof. J.C. Hunziker for being initiators of this study, as well as for their support. We are greatly indebted to Dr. L. Marini for his useful advice and constructive comments. Prof. M. Burkhard and Prof. G. Menard are greatly thanked for their enthusiastic and pertinent reviews. We thank Dr. C. Williams for his suggestions and Prof. L. Rybach for their encouragements. We thank: Dr. T. Brombach, Dr. L. Calmbach, Prof. J.-L. Epard, Dr. M. Guidi, Prof. G. Martinotti, Prof. H.-R. Pfeifer, Prof. M. Sartori, Dr. Thélin and Dr. F. Vuataz, for the interesting discussions.

REFERENCES

Bianchetti, G., Zuber, F., Vuataz, F.-D. & Rouiller J.-D. 1993: Hydrolgeoligische und geothermische Untersuchungen im Simplontunnel. Matér. Carte Géol. Suisse, Série Géotech. 88, 1–75.

Bodmer, Ph., England, P. C., Kissling, E. & Rybach, L. 1979: On the correction of subsurface temperature measurements for the effects of topographic relief, Part II: Application to temperature measurements in the Central Alps. – In V. Čermák & L. Rybach (Eds.): Terrestrial Heat Flow in Europe. – Springer-Verlag, Berlin, Heidelberg, New York, pp. 78–87.

Bodri, L. & Rybach, L. 1998: Influence of topographically driven convection on heat flow in the Swiss Alps: a model study. Tectonophysics 291, 19–27.

Bowen, R. 1989: Geothermal resources. Elsevier. 484 pp.

Burbank, D. W. & Anderson, R. S. 2001:Tectonic Geomorphology. Balckwell Science, 274 p.

Burkhard, M. 1990: Aspects of large-scale Miocene deformation in most external part of Swiss Alps (Subalpine Molasse to Jura fold belt). Eclogae Geol. Helv. 83, 559–583.

Busslinger, A. 1998: Geothermische Prognosen für tiefliegende Tunnel. Ph.D thesis ETH Zürich.

Busslinger, A., Rybach, L. 1999a: Geothermal prediction of water-bearing zones. Tunnel 1, 33–41.

Busslinger, A., Rybach, L. 1999b: Prediction rock temperatures for deep tunnels. Tunnel 1, 25–32.

Carslaw, H.S. & Jaeger, J.C. 1959: Conduction of heat in solids. Oxford University press, 510 pp.

Čermák, V. & Bodri, L. 1996: Time-dependent crustal temperature modeling: Central Alps. Tectonophysics 257, 7–24.

Clark, S. P. Jr. & Niblett, E.R. 1956: Terrestrial heat flow in the Swiss Alps. The Geophysical J. Royal Astro. Soc. 7, 176–195.

Crank, J. 1975: The mathematics of diffusion. Calderon Press, 414 p.

Deichmann, N. 1992: Structural and rheological implications of lower-crustal earthquakes below northern Switzerland. Phys. Earth Planet. Inter. 69, 270–280.

Deichmann, N., Baer, M., Ballarin, D., Fäh, D., Flück, P., Kastrup, U., Kradolfer, U., Künzle, W., Mayer-Rosa, D., Röthlisberger, S., Schler, T., Sellami, S., Smit, P. & Giardini, D. 1998: Earthquakes in Switzerland and surrounding regions during 1997. Eclogae Geol. Helv. 91, 237–246.

Escher, A. & Beaumont, C. 1997: Formation, burial and exhumation of basement nappes at crustal scale: a geometric model based on the Western Swiss-Italian Alps. J. Struct. Geol. 19, 955–974.

Escher, A., Hunziker, J. C., Marthaler, M., Masson, H., Sartori, M. & Steck, A. 1997:. Geologic framework and structural evolution of the Western Swiss-Italian Alps. In: Pfiffner, O.A., Lehner, P., Heitzmann, P., Mueller, S., Steck, A. (Eds.): Deep structure of the Swiss Alps (Results of the NRP 20), 205–221.

Grasemann, B. & Mancktelow, N.S. 1993: Two-dimensional thermal modelling of normal faulting; the Simplon fault zone, Central Alps, Switzerland. Tectonophysics 225, 155–165.

Gudefin, H. 1967: Observations sur les venues d'eau au cours du percement du tunnel sous le Mont-Blanc Bull. BRGM Sec. 2 Geol. Appl. Chronique des Mines. 4, 95–107.

Hunziker, J. C., Martinotti, G., Marini, L. & Principe., C. 1990:. The waters of the Simplon Tunnel (Swiss- Italian Alps) and of the ajacent Ossola district (Italy): geothermal considerations. Geothermal Resources Council Transactions 14–II, 1477–1482.

Incropera, F. P., & De Witt, D.P. 1996: Fundamentals of heat and mass transfer. John Wiley & Sons, 886 pp.

Jaboyedoff, M. 2000: Modèles thermiques simples de la croûte terrestre: un regard sur les Alpes. Bull. Soc. Vaud. Sci. Nat. 86, 229–271.

Jaboyedoff, M. & Pastorelli, S. 1999: The present state of Alpine region : Influence of fluid circulation. Eur. Geother. Conf. Basel 99 Proc. 2, 177-187.

Kahle, H. G., Geiger, A., Buerki, B., Gubler, E., Marti, U., Wirth, B., Rothacher, M., Gurtner, W., Beutler, G., Bauersima, I. & Pfiffner, O. A. 1997: Recent crustal movements, geoid and density distribution; contribution from integrated satellite and terrestrial measurements. In: Pfiffner, O.A., Lehner, P., Heitzmann, P., Mueller, S., Steck, A, (Eds.), Deep structure of the Swiss Alps (Results of the NRP 20), 251–259.

Kukkonen, I. T. & Clauser, C. 1994: Simulation of heat transfer at the Kola deep-hole site; implications for advection, heat refraction and palaeoclimatic effects. Geophys. J. Int. 116, 409–420.

Mancktelow, N. S. & Grasemann, B. 1997: Time-dependent effects of heat advection and topography on cooling histories during erosion. Tectonophysics 270, 167–195.

Maréchal, J. C. 1998: Les circulations d'eau dans les massifs cristallins alpins et leurs relations avec les ouvrages souterrains. Ph-D Thesis, Ecole Polytechnique Fédérale de Lausanne.

Martinotti, G., Marini, L., Hunziker, J. C., Perello, P. & Pastorelli, S. 1999: Geochemical and geothermal study of springs in the Ossola-Simplon Region. Eclogae Geol. Helv. 92, 295–305.

MAURER, H. R., BUCKHARD, M., DEICHMANN, N. & GREEN, A.G. 1997: Active tectonism in the Central Alps; contrasting stress regimes North and South of the Rhone Valley. Terra Nova 9, 91–94.

MEDICI, F. & RYBACH, L. 1995: Geothermal map of Switzerland 1995 (heat flow density). Mater. Geol. Suisse Geophys., 30 pp.

OKAYA, N., FREEMAN, R., KISSLING, E. & MUELLER, ST. 1996: A lithospheric cross-section through the Swiss Alps – I. Thermokinematic modelling of the Neoalpine orogeny. Geophys. J. Int. . 125, 504–518.

OXBURGH, E. R. & ENGLAND, P. C. 1980: Heat flow and the metamorphic evolution of the Eastern Alps. Eclogae Geol. Helv. 73, 379–398.

PASTORELLI, S., MARINI, L. & HUNZIKER, J. 2000: Chemistry, isotope values (δD, $\delta^{18}O$, $\delta^{34}S_{SO4}$) and temperatures of the water inflows in two Gotthard tunnels, Swiss Alps. Appl. Geoch, 16, pp. 633–649. ()

PASTORELLI, S. 1999: Low enthalpy resources of the Western Alps. Geochemistry and isotopic considerations and tectonic constraints. Example of the cantons of Ticino and Bern (Switzerland). PhD Thesis Univ. Lausanne. 149 pp.

PAVONI, N. 1977: Erdbeben im Gebiet der Schweiz Eclogae Geol. Helv. 70, 351–370.

PEACOCK, S. M. 1989: Thermal modelling of metamorphic pressure-temperature-time paths : a forward approach. In SPEAR, S., PEACOCK, S.M. (Eds.) Metramorphic Pressure-Temperature-Time Paths AGU. Short Course in Geol 7, 57–102.

PINET, P. & SOURIOT, M. 1988: Continental erosion and large-scale relief. Tectonics, 3, 563–582.

POPOV, Y. A., PEVZNER, S. L., PIMENOV, V.P. & ROMUSHKEVICH, R.A. 1999: New geothermal data from the Kola super deep well SG-3. Tectonophysics pp. 306: 345–466.

ROY, R.F., BECK, A.E. & TOULOUKIAN, Y.S. 1981: Thermophysical Properties of rocks. In: TOULOUKIAN, Y.S., JUDD, W.R., ROY, R.F. (Editors). Physical properties of rocks and minerals, Mc Graw-Hill, 409–502.

ROZANSKI, K., ARAGUAS-ARAGUAS, L. & GONFIANTINI, R. 1993: Isotopic patterns in modern global precipitations. In: SWART, P. K., LOHMANN, K. C., MCKENZIE J. A. & SAVIN S. (Eds.) Climate change in continental isotopic records. AGU Monograph. 78, 1–36.

RYBACH, L. 1981: Geothermal systems, conductive heat flow, geothermal anomalies. In: RYBACH, L., MUFFLER, L.J.P., (Editors), Geothermal systems principles and case histories, John Wiley & Sons : 3–36.

RYBACH, L. 1995: Thermal waters in deep Alpine tunnels. Geothermics 24, 631–637.

RYBACH, L., BODMER, P., WEBER, R. & ENGLAND, P. C. 1982: Heat flow and heat generation in the new Gotthard tunnel, Swiss Alps (preliminary results). In: ČERMÁK, V., HAENEL, E., (Eds.), Terrestrial heat flow in Europe Geothermics and geothermal energy, Schweitzerbart'sche Verlagsbuchh., Stuttgart, 63–69.

RYBACH, L. & PFISTER, M. 1994: How to predict rock temperature for deep Alpine tunnels. J. Appl. Geophys. 31, 261–270.

SEWARD, D. & MANCKTELOW, N. S. 1994: Neogene kinematics of the Central and Western Alps; evidence from fission-track dating. Geology 22, 803-806.

SIBSON, R.H. 1977: Fault rocks and fault mechanisms. J. Geol. Soc. London 133, 191–213.

SMITH, L. & CHAPMAN, D.S. 1983: On the thermal effects of groundwater flow. J. Geophys. Res. B 88, 593–608.

STAMPFLI, G.M., MOSAR, J., MARQUER, D. & MARCHANT, R. 1998: Subduction and obduction process in the Swiss Alps. Tectonophysics, 296, 159–204.

STECK, A. & HUNZIKER, J. 1994: The Tertiary structural and thermal evolution of the Central Alps – compressional and extensional structures in orogenic belt. Tectonophysics 238, 229–254.

TURCOTTE, D. L. & SCHUBERT, G. 1982: Geodynamics; applications of continuum physics to geological problems. John Wiley & Sons, 450 pp.

VANCE, D. & O'NIONS, K. 1992: Prograde and retrograde thermal histories from central Swiss Alps. Earth Planet. Sci. Lett. 114, 113–129.

VUATAZ, F. D. 1982: Hydrogéologie, géochimie et géothermie des eaux thermales en Suisse et des régions limitrophes. Soc. Helv. Sci. Nat. 29, 1–174.

VUATAZ, F. D. 1997 : Natural variations in human influences on thermal water resources in the Alpine environment. Proceeding 33th Conf. Int. Soc. Hydrothermal Tech., Hakone Japan.

WENK, E. & WENK, H. R. 1984: Distribution of plagioclase in carbonate rocks from tertiary metamorphic belt of central Alps. Bull. Mineral. 107, 357–368.

Manuscript received December 11, 2001
Revision accepted September 7, 2002